

Design and analysis of heat transfer on a customized eco-print batik steamer with automatic temperature and time control using Computer Fluid Dynamic (CFD)

Handini Novita Sari^{1*}, *Rizal Mahmud*², *Nur Aini Susanti*³, *Imami Arum Tri Rahayu*⁴, *Susi Tri Umaroh*³, and *Agung Prijo Budijono*¹

¹Universitas Negeri Surabaya, Mechanical Engineering Department, Surabaya, Indonesia.

²Meiji University, Mechanical Engineering Informatics Department, Tokyo, Japan.

³Universitas Negeri Surabaya, Mechanical Engineering Education Department, Surabaya, Indonesia.

⁴Universitas Negeri Surabaya, Fashion Education Department, Surabaya, Indonesia.

Abstract. The process of making eco-print batik carried out by eco-print batik industry players still uses conventional methods with steaming pans. The conventional method used has a quite crucial impact on the equipment used, the bottom of the pan is susceptible to damage because it is used continuously for quite a long time. To overcome this problem, a steamer design will be created specifically for eco-print batik using Solid Work software. Following the completion of the design, this research investigates how the heat transfer process occurs, the circumstances of the heat flux created, and the temperature during the heating process using computer fluid dynamics (CFD) with simulation methods as an approach to real conditions. Observations were made in 300s, 600s, 900s, 1200s. The steamer material employed in this simulation is stainless steel 304, and the simulation results show that the steamer's heating temperature is. Based on the simulation results of high pressure in closed system conditions and the influence of materials with good thermal conductivity on the steamer, which have an impact on increasing temperature and heat flux during the process, through these considerations, the steamer is designed to be equipped with temperature control and a safety valve which functions to release pressure. steam when excessive. In this way, the steamer will be more effective and efficient in terms of time, heating, and the quality of the batik results that will be produced later when compared to the pan used previously.

1 Introduction

This eco-print batik is one type of batik whose manufacturing method utilizes natural dyes from tannins or dyes of leaves, roots or stems placed on a piece of cloth, then the cloth is boiled. Boiling this cloth takes approximately two hours to get perfect results. So

* Corresponding author: handinisari@unesa.ac.id

far, the eco-print batik boiling process carried out by eco-print batik industry players still uses conventional methods, namely using ordinary boiling pots. During the boiling process, temperature, pressure, and time conditions are not controlled when using conventional methods. The conventional method used has a crucial impact on the equipment used, for example, in the pan, the bottom of the pot is vulnerable to damage because it is used continuously for a long duration of time. In addition, the fabric bending treatment so that all the cloth put in the pot is sufficiently accommodated will damage the pattern that appears on the batik, the impact of this results in crease marks from the bend. In this conventional method, one pot can only hold one to two batik cloths, so in this case, it is inefficient in terms of time and quantity which will also have an impact on the consumption of fuel used during the production process.

The steamer design made specifically for batik eco-print will be equipped with temperature and time control so that the process of boiling batik eco-print fabric can run without interference from uncontrolled temperature and time conditions so that users can easily adjust the conditions according to their individual needs. The steamer will be designed with material that is sturdier and more reliable using materials that have high heat resistance. The capacity or capacity of the steamer will also be calculated according to needs so that it will be more effective and efficient in terms of time with a larger input quantity than before.

The first step taken in this research is to make an eco-print batik steamer design with solid work software. After the design is completed, this study will also examine how the heat transfer process takes place, how the heat flux conditions are produced, the maximum temperature obtained, and the convection coefficient during the heating process. In this case, using computer fluid dynamics (CFD) with simulation methods as an approach to real conditions. One of the most effective methods for assessing and managing superheater models is computational fluid dynamics (CFD), which enables study of extremely complex geometries while taking into consideration the intricacies of three-dimensional geometric models [1] [2]. It is also feasible to measure the heat transfer between exhaust gases and steam during superheater operation, as well as the heat transfer coefficient on both the steam and the hot side of the superheater [3].

Research related to the phenomenon of heat transfer, condensation, evaporation and material treatment of tools that use stainless steel material has been carried out both experimentally and simulated, such as research conducted by [4]. The purpose of this research is to determine how the initial temperature of the substrate affects the heat transmission, microstructure, hardness, and residual stress of AISI 316 L stainless steel deposits on AISI 304 steel substrates. Perhaps the methods presented here might be applied to further additive manufacturing research in alloys and other metal equipment, bringing reliability and durability to additive manufacturing (AM). Wei Li described condensation heat transfer in annuli outside the enhanced horizontal stainless steel tube, which he claims is commonly used to improve heat transmission in various scenarios [5]. One of the primary processes that occurs in energy conversion systems is boiling heat transfer. Arcasi research et. al. [6] discuss the experimental examination of hysteresis phenomena during boiling stream heat transfer in horizontal stainless steel. The relative influence of neighboring cavities is still a topic of theoretical debate in the literature today [7], from numerical [8], and experimental [9] points of view.

Tests performed under the same operating conditions but with different thermal histories (heat flux charged greater in the transient phase) are thought to be influential in giving the wall a lower superheat value and hence higher heat transfer performance. The boiling theory eventually enforced the experimental trend, taking into account the effect of hysteresis as the activation of surface cavities subjected to higher temperature boundary conditions. In the study of H.E. Zhang et al., a CFD model was built to mimic the entire process of directional energy deposition of stainless steel. To investigate physical phenomena associated with this process, such as temperature behavior, melt flow characteristics, and layer growth, systematic simulations of melt ponds and deposited layers are used [10]. Process parameters, sample characteristics, and DED process modeling are all examples of DED process modeling. Particle ejection studies reveal that a number of elements, such as coaxial nozzle shape, inert gas flow rate, and particle characteristics, do have a significant impact on powder flow [11-15]. With a steady stream of powder, the ejected particles heat the focused laser beam falling into the melt pond and are considered an additional mass [16-18]. In addition, clad formation is also directly affected by the size and temperature of the melt pool [19, 20]. As a result, it is vital to better understand how the melt pool evolves and how it influences clad formation. According to Asghar Hozoorbakhsh et al.'s study on An investigation of heat transfer and fluid flow on laser micro-welding upon the thin stainless steel sheet (SUS304) using computational fluid dynamics (CFD) [21].

2 Methods

The method used in this study is computer fluid dynamic (CFD) which is a simulation method to analyze heat transfer studies that occur when the steamer is used for the batik fabric steamer process. The complete design of the steamer is shown in Figure 1.

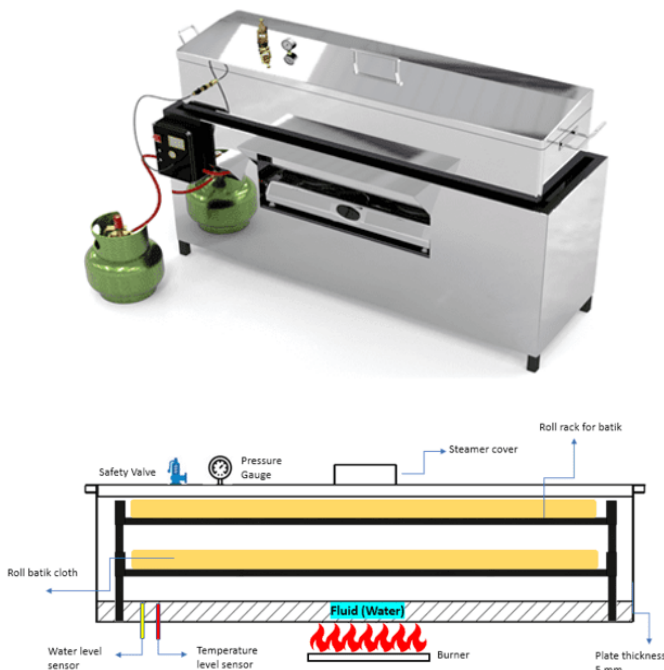


Fig. 1. Eco-print batik steamer desi

2.1 Modelling heat and mass transfer

2.1.1 Heat transfer

Heat transfer in fabrics is assumed based on the equation of Eq. (1) [22, 23].

$$\rho_m c_{pm} \frac{\partial T}{\partial t} + \nabla \cdot (-k_m \nabla T) + \rho_w c_{pw} u_w \nabla T = 0 \quad (1)$$

Where ρ_m and ρ_w are the densities of cloth and water (kg/m³), respectively. k_m is the thermal conductivity of the fabric (W/(m °C)), and is the heat capacity of the fabric and water (J/(kg °C)), u_w is the fluid velocity (m/s), T is the temperature (°C) and t is time (s).

2.1.2 Mass transfer

Based on the mass conservation formula and based on the equation of water transport with product given by equation (2) [22]

$$(\partial C)/\partial t + \nabla \cdot (Cu_w) = \nabla \cdot (D\nabla C) \quad (2)$$

where C represents the moisture concentration (kg of water/kg of sample), t is time(s), u_w is the velocity of the fluid (m/s) and D is the moisture diffusion coefficient (m²/s)

2.2 Boundry and initial condition

The convective heat flux from the hot air to the surface of the product is given by eq. (3) [22].

$$q = h (T_{\text{steamer}} - T_s) \quad (3)$$

Where q is the heat flux convective flux (W/m²), h is the heat transfer coefficient average (W/(m²°C)), T steamer is the temperature of the steamer (°C) and T s is the surface temperature of the product (fabric) (°C).

2.2.1 Heat transfer boundary condition

The heat flux boundary condition is given by eq. 4

$$(1-f) h (T_{\text{steamer}} - T_s) = -n (k_m \nabla T + \rho_w c_{pw} u_w T) \quad (4)$$

f is the fraction of energy lost by evaporation of water on the surface. The value of f is between 0 and 1. The parameter f is viewed as an empirical switching function that

determines how much of the provided energy is utilized for evaporation. $T_s \geq 100 \text{ }^\circ\text{C}$ predominates during evaporation, and f quickly climbs to values closer to 1 than to 0. The precise value of f will be determined by the conditions of heat transmission and mass loss, and it should be calculated at this stage through trial and error. Mass transfer boundary condition. The mass flux boundary condition is given by eq. 5.

$$n \cdot (-DVC + u_w C) = f h \frac{(T_{\text{steamer}} - T_s)}{H_{\text{evap}} \rho} (C - C_{\text{eq}}) \tag{5}$$

2.2.2 Initial condition

$$T = T_0 \text{ and } C = C_0$$

2.3 Experiment setup

The material used as the basic material of the steamer is stainless steel 304, the use of this material is based on the consideration that stainless steel type 304 is a versatile type of stainless steel. Its chemical composition, mechanical strength, weldability, and corrosion resistance are excellent at a relatively affordable price. Stainless steel type 304 is widely used in the industrial world and small scale. The complete input parameters of the material are shown in Table 1, as well as the water properties shown in Table 2.

Table 1. The input parameters material steamer SS304

Properties of Outline Row 5: Steel Stainless 304			
	A	B	C
1	Property	Value	Unit
2	Material Field Variables	Table	
3	Density	8055	kg m ⁻³
4	Isotropic Thermal Conductivity	16,2	W m ⁻¹ C ⁻¹
5	Specific Heat	500	J kg ⁻¹ C ⁻¹

Table 2. Water property

Properties of Outline Row 7: Water Fresh			
	A	B	C
1	Property	Value	Unit
2	Material Field Variables	Table	
3	Density	997,4	kg m ⁻³
4	Isotropic Thermal Conductivity	0,604	W m ⁻¹ C ⁻¹
5	Specific Heat	4179	J kg ⁻¹ C ⁻¹

Table 3. Material of Burner: Brass

Properties of Outline Row 3: Brass			
	A	B	C
1	Property	Value	Unit
2	Density	8600	kg m ⁻³
3	Isotropic Thermal Conductivity	111	W m ⁻¹ C ⁻¹
4	Specific Heat	162	J kg ⁻¹ C ⁻¹

The image below is an illustration of the boundary conditions of an eco-print batik steamer which is simulated running in closed system conditions.

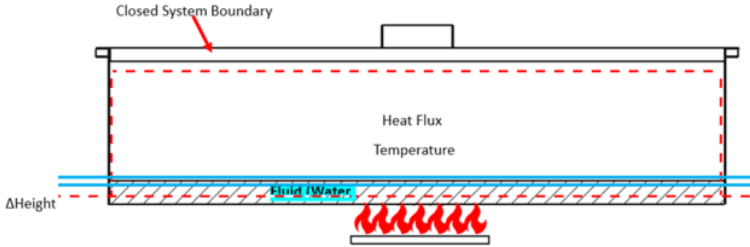


Fig. 2. Boundary layer condition

Input for Simulation Parameters:

1. Temperature of Heat Source
2. Film Coefficient of Water
3. Bulk Temperature
4. Time Variation [300s, 600s, 900s, 1200s, 1500s]
 (to check water evaporation/5 minutes)

Objective:

1. Temperature Distribution (T)
2. Heat Flux Distribution (Q)

2.4 Meshing

The meshing process is one of the important processes in CFD, the quality of the mesh greatly determines the output results of the simulation. Meshing is the process of dividing a domain into several cells. In general, mesh is divided into 2, namely mesh with a structured grid and mesh with an unstructured grid. The general scalar equation used in the discretization process is. Place the figure as close as possible after the point where it is first referenced in the text. If there is a large number of figures and tables, it might be necessary to place some before their text citation.

$$\underbrace{\frac{\partial(\rho\phi)}{\partial t}}_{\text{transient term}} + \underbrace{\nabla \cdot (\rho\mathbf{u}\phi)}_{\text{convection term}} = \underbrace{\nabla \cdot (\Gamma\nabla\phi)}_{\text{diffusion term}} + \underbrace{\underline{Q}}_{\text{source term}}$$

$$\underbrace{\frac{\partial(\rho\phi)}{\partial t}}_{\text{transient term}} + \underbrace{\frac{\partial(\rho u\phi)}{\partial x} + \frac{\partial(\rho v\phi)}{\partial y}}_{\text{convection term}} = \underbrace{\frac{\partial}{\partial x} \left(k \frac{\partial\phi}{\partial x} \right) + \frac{\partial}{\partial y} \left(k \frac{\partial\phi}{\partial y} \right)}_{\text{diffusion term}} + \underbrace{\underline{Q}}_{\text{source term}} \quad (6)$$

By dividing the work area into cells, the discretization process can be carried out, so that the CFD calculation process can be carried out, but in CFD the approach can be carried out with finite differences or finite volumes, after the calculation/iteration process

is carried out until convergent results are obtained, the respective values The points will be known, so that the values of these points can be displayed, either through an attractive GUI visualization, or simply numerical data in a table.

Figure 3 is the result of meshing from an eco-print batik steamer. The average skewness value of the meshing steamer is 0.47865 while the minimum skewness is 1.3057e-010, meaning that the meshing quality can be said to be very good.

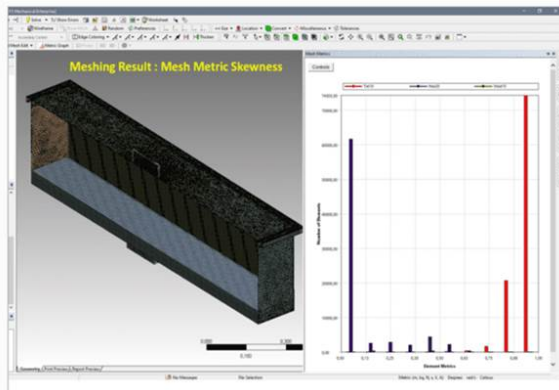


Fig. 3. Meshing of steamer

3 Result and discussion

3.1 Temperature distribution

Figure 4 depicts the modeling results of the temperature distribution of the eco-print batik steamer made of 304 stainless steel. Where significant temperature differences are depicted, at the heat source the temperature was set at 120 °C, and simulation observations were carried out at $t=300s$ to $t=1200s$. As time goes by, overall heat propagation occurs both vertically and horizontally. At $t=300s$ to $t=1200s$, the bottom of the steamer temperature shows a figure of around 118.79–120.5 °C, where the steamer is filled with 28.32 liters of water with a fluid height of around 59 mm. The temperature distribution in the steamer section containing fluid is at $t=300s$ to 900s in the temperature range of 102.93–117.1 °C, with an average temperature of 109.878 °C. At $t=1200s$ the average fluid temperature shows an increase of 110.174 °C. This means that at $t=300s$ the fluid has reached the boiling point of water. In theory, water will boil at a temperature of 100 degrees Celsius at a pressure of 1 atmosphere. Because the steamer is made of thick and strong stainless steel and has a tight lid, the water vapor produced during the boiling process cannot possibly escape and only collects in the steamer. This collected water causes the water pressure in the steamer to rise, which causes the boiling temperature to also rise to 100 °C.

At $t=300s$, 600s, and 900s the average fluid temperature is the same, this is because the observation time distance is too close, and the cross-sectional area and water volume are quite large which also influences the convection heat transfer process that occurs in the fluid. The surface that has a higher heat load will transmit heat, in this case, the density of the lower water decreases, so the water particles are pushed to the surface of the steamer, and their place is automatically replaced by water which falls to the bottom of the lower surface until the water boils.

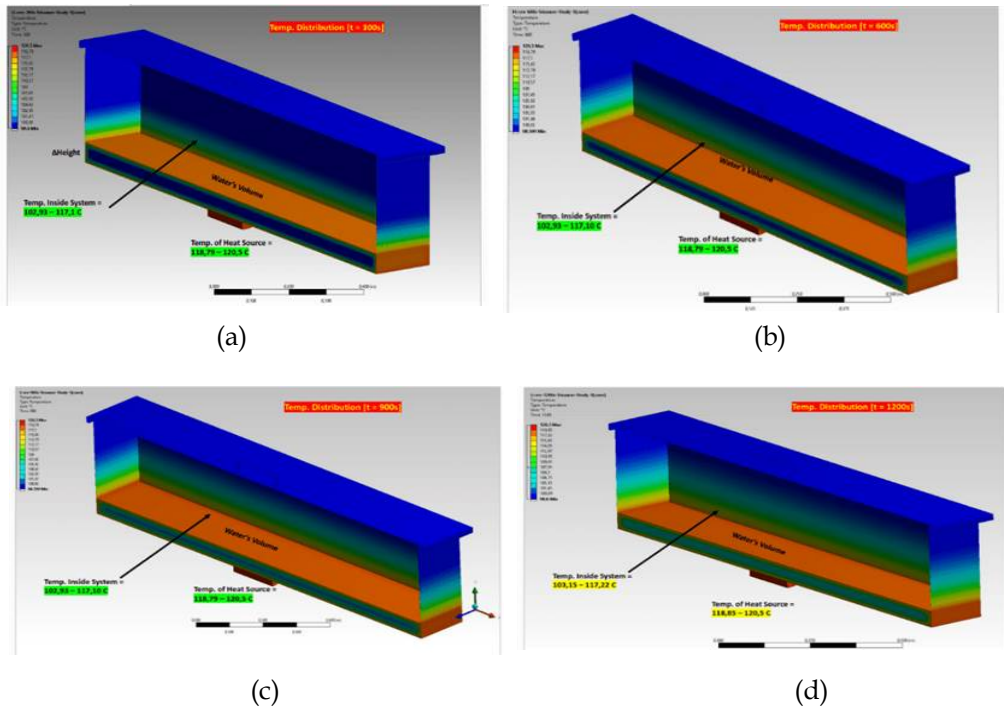


Fig. 4. Temperature distribution at time (a) 300s, (b) 600s, (c) 900s, and (d) 1200s

3.2 Heat Flux

The heat flux condition at $t=300s$ in the fluid is in the range 2.133-357.11 W/m² with the water volume reduced to 28.32 liters from the initial volume of 28.77 liters. At $t=600$ to 900s, the heat flux value in the fluid is in the range 8,467-718,920 W/m², and at $t=1200s$ the heat flux value in the fluid is 12,867- 876.96 W/ m². From Figure 5 we can see that the heat flux increases with increasing temperature and time. Meanwhile, the volume of water also decreased frequently with increasing temperature and time, respectively amounting to 27.63 liters, 26.88 liters, and 26.16 liters.

Because this steamer works in a closed system, as a safety measure, the steamer is provided with a safety valve that functions to release steam pressure when it is excessive. This is because the steamer uses a tight lid so that water vapor cannot escape. At a certain time, this tool reaches the threshold or standard for the start of calculating the cooking time, which is marked by a hissing sound due to water vapor passing through the safety valve. So it can be concluded that the process of steaming eco-print batik cloth using this steamer can be faster than using a regular pan because the heat absorbed by the trapped steamer cannot come out again (closed system) so the pressure inside the steamer rises along with the temperature rise and no change in volume occurs. Init (isochoric process) or there is only a slight reduction in water due to the presence of the safety valve. The aim of the steaming process for eco-print batik cloth is to bring out the basic color of the leaves so that it can produce a beautiful pattern of fine cloth.

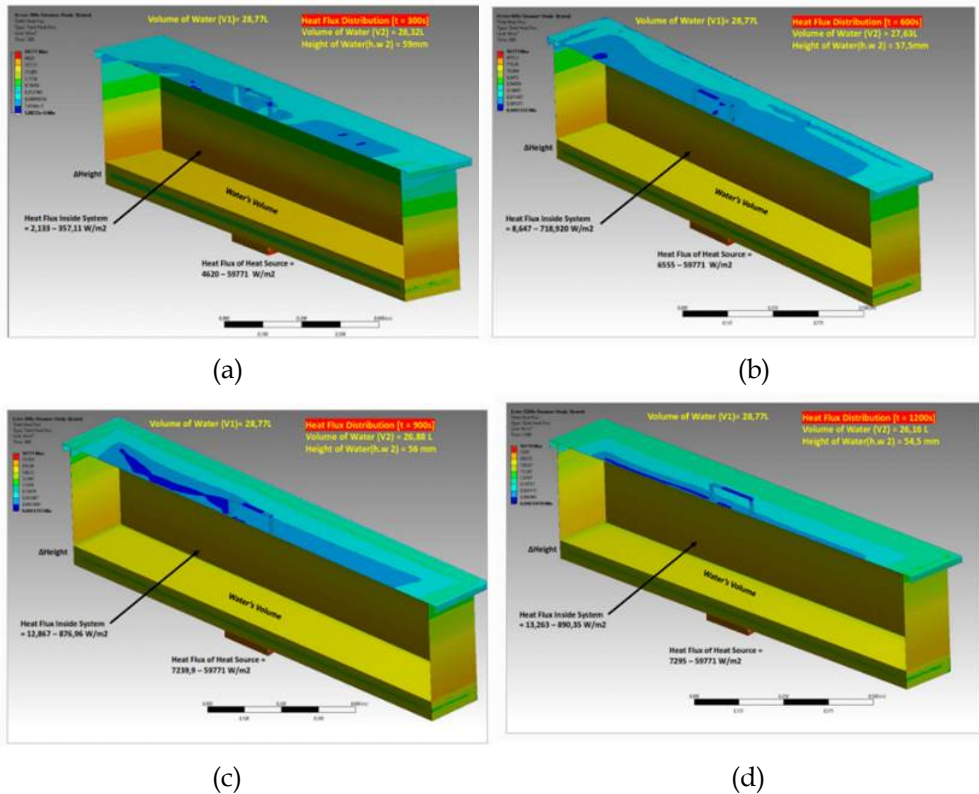


Fig. 5. Heat flux of steamer at t (a) 300s, (b) 600s, (c) 900s, and (d) 1200s

The high pressure in closed system conditions and the influence of materials with good thermal conductivity on the steamer, have an impact on increasing temperature and heat flux during the process, so through these considerations, the steamer is designed to be equipped with temperature control. This temperature control functions to make it easier for users to adjust temperature control. Based on research conducted by Entien Darmawati and Sutopo who examined the effect of steaming temperature for eco-print batik cloth on color sharpness and fastness, it was concluded that the most optimal temperature was in the range of 70-80 °C [24]. With this temperature control, the temperature conditions to get the best quality from eco-print batik can be maintained.

4 Conclusion

Based on results and discussion, it can be concluded that : (1) The temperature distribution in the steamer section containing fluid is at t=300s to 900s in the temperature range of 102.93-117.1 °C, with an average temperature of 109.878 °C. At t=1200s the average fluid temperature shows an increase of 110.174 C. This means that at t=300s the fluid has reached the boiling point of water ; (2) Heat flux at t=300s in the fluid is in the range 2.133-357.11 W/m² with the water volume reduced to 28.32 liters from the initial volume of 28.77 liters. (3) At t=600 to 900s, the heat flux value in the fluid is in the range of 8,467-718,920 W/m², and at t=1200s the heat flux value in the fluid is 12,867-876.96 W/m². The high pressure in closed system conditions and the influence of materials with good thermal conductivity on the steamer, have an impact on increasing temperature and heat flux during the process, so through these considerations, the steamer is designed to be equipped with temperature control and a safety valve which functions to release steam pressure when excessive.

References

1. T. D. Granda, M. Trojan, *Energy* **199**, 117423 (2020)
2. P. Ludowski, D. Taler, J. Taler, *Appl Therm Eng.* **58** (2013)
3. P. Madejski, D. Taler, A. Korzeń, *Arch. Energ.* **3** (2012)
4. D. V. Isquierdo, R. H. M. Siqueira, S. M. Carvalho, M. S. F. Lima, *J. Mater. Res. Technol.* **18** (2022)
5. W. Li, H. Chen, J. Wang, Y. Gao, X. Wang, *Int. J. Therm. Sci.* **177** (2022)
6. A. Arcasi, R. Mastrullo, A. W. Mauro, L. Viscito, *Int. J. Heat Mass Transf.* **164** (2021)
7. S. Ming-Heng, J. Ma, W. Bu-Xuan, *Int. J. Heat Mass Trans.* **36** (1993)
8. N. B. R. Mallozzi, R. L. Judd, *Int. J. Heat Mass Transf.* **43** (2000)
9. R. L. Judd, *J. Heat Transf.* **110** (1988)
10. Y. M. Zhang, C. W. J. Lim, C. Tang, B. Li, *Int. J. Therm. Sci.* **165** (2021)
11. S.Y. Wen, Y.C. Shin, J.Y. Murthy, P. E. Sojka, *Int. J. Heat Mass Transf.* **56**, 25–26 (2009)
12. A. J. P. J. Ibarra-Medina, *Phys. Procedia* **5** (2010)
13. H. Liu, X. L. He, G. Yu, Z. B. Wang, S. X. Li, C. Y. Zheng, W. J. Ning, *Sci. China Physics, Mech. Astron.* **58** (2015)
14. G. F. J. Yan, I. Battiato, *Int. J. Adv. Manuf.* **91**, 1–4 (2016)
15. O. B. Kovalev, I. O. Kovaleva, I. Y. Smurov, *J. Mater. Process. Technol.* **249** (2017)
16. J. Ibarra-Medina, *Development and Application of a CFD Model of Laser Metal Deposition* (University of Manchester, Manchester, 2012).
17. I. Taberner, A. Lamikiz, S. Martínez, E. Ukar, *Phys. Procedia* **39** (2012)
18. I. Arrizubieta, A. Lamikiz, F. Klocke, S. Martínez, K. Arntz, *Int. J. Heat Mass Transf.* **115** (2017)
19. X. Wang, et al., *Research on remelting phenomena and metal joining of fused-coating additive manufacturing*, in *Journal of Physics: Conference Series*, 1063, IOP Publishing (2018)
20. J. Du, X. Wang, H. Bai, G. Zhao, Y. Zhang, *International Journal of Thermal Sciences* **114** (2017)
21. A. Hozoorbakhsh, M. I. S. Ismail, A. A. D. M. Sarhan, A. Bahadoran, N. B. A. Aziz, *Int. Commun. Heat Mass Transf.* **75** (2016)
22. E. Bird, W. Stewart, E. Lightfoot, *Transport phenomena* (John Wiley and Sons, New York, 2001).
23. R. G. M. Van der Sman, *Meat Sci.* **76**, 4 (2007)
24. E. Darmawati, *Berkala Penelitian Teknologi Kulit, Sepatu, dan Produk Kulit* **20**, 1 (2021)